23–27
June 2013

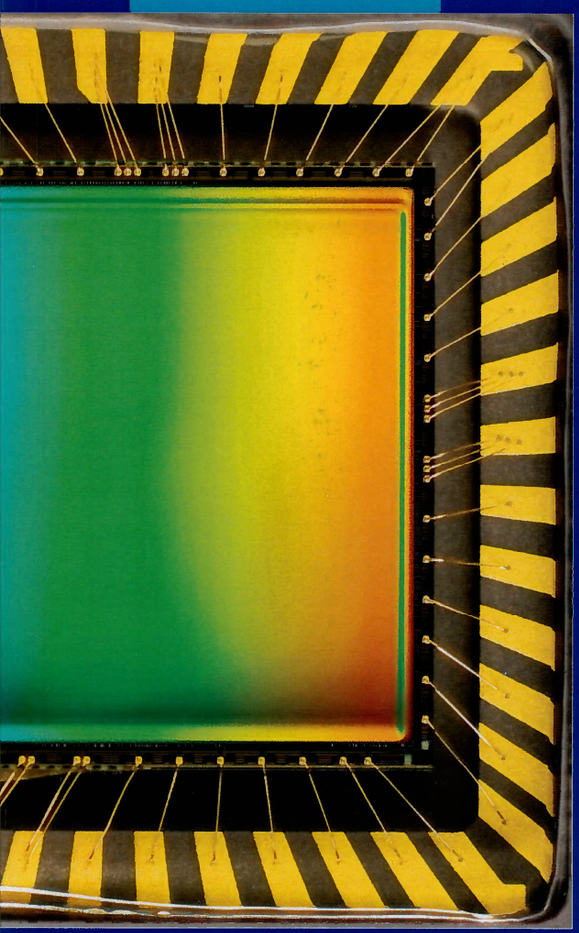

Conference Program

Imaging and Applied Optics

OSA Optics & Photonics Congress

Adaptive Optics: Methods, Analysis and Applications (AO)

Applied Industrial Optics: Spectroscopy, Imaging & Metrology (AIO)

Computational Optical Sensing and Imaging (COSI)

Fourier Transform Spectroscopy (FTS)

Imaging Systems and Applications (IS)

Propagation Through and Characterization of Distributed Volume Turbulence (pcDVT)

Quantitative Medical Imaging (QMI)

Renaissance Arlington Capital View
Arlington, Virginia, USA

OSA®

www.osa.org/imaging_congress

These concurrent sessions are grouped across two pages. Please review both pages for complete session information.

OTu3A • AO Performance Metrics Discussion —Continued

AO has become increasingly commonplace across a diverse range of applications. Maturation of AO methods along with technology developments have pushed the performance limits of both laboratory based and commercial AO systems. With these developments there is increasing need for simple, yet effective metrics to assess AO performance. This is particular pressing for commercial applications, as for example in clinical ophthalmology, where the systems are operated by non-technical personnel. While different applications may require different AO metrics, use of the same AO fundamentals suggest there may also be much commonality. These issues will be explored in this session through a panel led discussion of leading AO experts. Please come with your own AO metric questions for the panel.

ATu3B • LIDAR - Applications and Innovations—Continued

ATu3B.2 • 15:10 Invited

New Inversion Algorithms for Multi-Angle Lidar, Gary G. Gimmestad[1], David Roberts[1]; *[1]Electro-Optical Systems Laboratory, Georgia Tech Research Inst., USA.* New algorithms are shown for inverting data from angle-scanning lidars. In contrast to algorithms for finding the atmospheric extinction coefficient, the new algorithms find the range-dependent atmospheric transmittance. Great simplifications result from this new approach.

ATu3B.3 • 15:50 Invited

Space lidars and Interplanetary Laser Ranging and Communication Experiments Performed by NASA GSFC, Xiaoli Sun[1]; *[1]Laser Remote Sensing Lab, NASA Goddard Space Flight Center, USA.* NASA Goddard Space Flight Center (GSFC) has developed a series of space lidar and successfully mapped Mars, Earth, Mercury and Moon. Interplanetary laser ranging and communications were also conducted from Earth to these space lidar.

CTu3C • Phase Imaging II—Continued

CTu3C.2 • 15:10

Phase Retrieval for Time Resolved Dual-Detector Microtomography with Partially Coherent X-rays, Martin Nyvlt[1,2], Marek Skeren[1], Marco Stampanoni[2], Rajmund Mokso[2]; *[1]Czech Technical Univ. in Prague, Czech Republic; [2]Swiss Light Source, Paul Scherrer Institut, Switzerland.* To overcome the limited contrast to noise ratio in fast time resolved 4D imaging with partially coherent X-ray, we propose new options of phase retrieval with a dual-detector acquisition scheme. An iterative refinement of the phasing methods is evaluated

CTu3C.3 • 15:30

Phase retrieval using constrains derived from the Helmholtz equation, Mostafa A. Agour[1,2], Ervin Kolenovic[3], Claas Falldorf[3], Christoph von Kopylow[1], Werner Jueptner[1], Ralf B. Bergmann[1]; *[1]BIAS, Germany; [2]Department of Physics, Faculty of Science, Egypt; [3]Syperion GmbH, Germany.* We present a new phase retrieval method which, similar to common temporal phase shifting, requires only four intensity measurements to recover the complex amplitude of arbitrary wave fields without the need for a priori knowledge.

CTu3C.4 • 15:50

Compressive Effects of Positivity in Coherence Retrieval, Zhengyun Zhang[1], George Barbastathis[1,2]; *[1]Singapore-MIT Alliance for Res & Tech Ct, Singapore; [2]Mechanical Engineering, Massachusetts Inst. of Technology, USA.* Positivity is often used in coherence retrieval to improve reconstruction fidelity and enforce physical plausibility of the result. We show that its use induces compressive sensing-like behavior when the mutual intensity matrix has low rank.

CTu3C.5 • 16:10

Snapshot conical diffraction phase image measurement in angle-resolved microellipsometry, Daesuk Kim[1,3], Moonseob Jin[1], Hyungchul Lee[2], Soohyun Kim[2], Robert Magnusson[3]; *[1]Chonbuk National Univ., Republic of Korea; [2]KAIST, Republic of Korea; [3]Univ. of Texas at Arlington, USA.* We describe a snapshot conical diffraction phase image measurement method in angle resolved microelliposometry. We expect the proposed scheme can be extended to digital holography based conical diffraction phase image extraction field.

FTu3D • Lab Experiment—Continued

FTu3D.2 • 15:10

Accurate laboratory atomic and molecular data for astrophysics applications by high resolution Fourier transform spectrometry, Juliet C. Pickering[1], Matthew Ruffoni[1], Florence Liggins[1], Anne P. Thorne[1]; *[1]Imperial College London, UK.* Accurate high resolution atomic and molecular data are required for interpretation of many astrophysical spectra. The Imperial College London laboratory astrophysics program using high resolution Fourier Transform spectrometry is described.

FTu3D.3 • 15:30

Development of an FTS-based Spectral Responsivity Comparator, Joseph P. Rice[1], Jorge Neira[1]; *[1]NIST, USA.* We have developed a method of measuring the absolute spectral responsivity of infrared detectors using a Fourier Transform Spectrometer (FTS) coupled to a liquid-helium-cooled Electrically-Substituted Bolometer (ESB) as a reference detector.

FTu3D.4 • 15:50

Performance of a cryogenic 21 meter-path Herriott cell vacuum coupled to a Bruker 125 HR system, Keeyoon Sung[1], Arlan W. Mantz[2], Mary Ann H. Smith[3], Timothy J. Crawford[1], ShanShan Yu[1], Linda R. Brown[1], D. Chris Benner[4], Malathy V. Devi[4]; *[1]Science Division, Jet Propulsion Lab./ Caltech, USA; [2]Dept. of Physics, Astronomy and Geophysics, Connecticut College, USA; [3]Science Directorate, NASA Langley Research Center, USA; [4]Dept. of Physics, The College of William and Mary, USA.* A cryogenic 21 meter-path Herriott cell designed for a broad-band Fourier transform infrared spectrometer, a Bruker 125HR, was recently developed at Connecticut Collage. The cell-interferometer system has excellent temperature and photometric stability over a wide temperature range.

FTu3D.5 • 16:10

Fiber probe for the spectral range of 2-45 μm for IR-Fourier spectrometer, Liya V. Zhukova[1], Alexandr S. Korsakov[1], Dmitry S. Vrublevsky[1], Andrey I. Chazov[1], Viktor S. Korsakov[1], Sergey V. Kortov[1]; *[1]Yeltsin UrFU, Russian Federation.* We worked out a fiber probe for FTS (2-45 μm). The fiber is extruded from new crystals based on silver and monovalent thallium halide solid solutions.

These concurrent sessions are grouped across two pages. Please review both pages for complete session information.

ITu3E • Military Applications—Continued

ITu3E.2 • 15:10
Rapid Focal Shifting Optics for Inline 3D Image Capture, Daniel C. Gray[1], Hongqiang Chen[1], Joseph Czechowski[1], Kevin Harding[1]; [1]*GE Global Research, USA.* We present a novel lens system with high-resolution and wide field-of-view for 3D image capture. A depth-from-defocus algorithm is implemented to reconstruct 3D object and matched with a fused image to create a 3D view.

ITu3E.3 • 15:30
Color Image Formation for Multiscale Gigapixel Imaging, Esteban Vera[1], Dathon R. Golish[1], Qian Gong[1], Kevin Kelly[1], David Kittle[2], Steve Feller[2], David J. Brady[2], Michael Gehm[1]; [1]*Univ. of Arizona, USA;* [2]*Duke Univ., USA.* We present the current development of the image formation pipeline for color gigapixel images obtained by the AWARE-10 multiscale camera. We introduce a camera simulator, the modifications to the scalable pipeline, and the challenges for creating seamless color gigapixel panoramas.

ITu3E.4 • 15:50
Capabilities of monocentric objective lenses, Igor Stamenov[1], Ilya P. Agurok[1], Joseph Ford[1]; [1]*Univ. of California San Diego, USA.* Monocentric lenses enable panoramic high-resolution imaging, but have not been fully explored. We present algorithms for systematic optimization of monocentric objectives, and show the tradeoff between lens complexity and focal length, numerical aperture and spectral bandwidth.

ITu3E.5 • 16:10
Adaptive digital holography for gain-enhanced imaging, Abbie T. Watnik[1], Paul S. Lebow[1]; [1]*US Naval Research Laboratory, USA.* An iterative feedback loop using a spatial light modulator provides wavefront shaping in a holography experiment. In addition to hardware components, an algorithmic technique to provide uniform illumination to the target prevents image oversharpening.

PTu3F • POAM—Continued

PTu3F.2 • 15:10
Detection of Orbital Angular Momentum in Optical Waves Propagating through Distributed Volume Turbulence, Denis W. Oesch[1], Darryl Sanchez[2], Anita Gallegos[1], Jason Holzman[2], Terry Brennan[3], Julie Smith[2], William Gibson[2], Tom C. Farrell[2], Patrick R. Kelly[2]; [1]*SAIC, USA;* [2]*AFRL, USA;* [3]*tOSC, USA.* We demonstrate the use of optical vortex trails in the identification of photonic orbital angular momentum in wave front sensor measurements of beams propagating through distributed volume turbulence.

PTu3F.3 • 15:30
The creation of photonic orbital angular momentum by molecular clouds, Darryl J. Sanchez[1], Denis W. Oesch[2], Patrick R. Kelly[1]; [1]*US Air Force Research Laboratory, USA;* [2]*SAIC, USA.* Here we establish that galactic atomic and molecular clouds create photonic orbital angular momentum (POAM). Then, summarize a set of on-sky experimental observations which corroborate the laboratory results.

PTu3F.4 • 15:50
Photonic Orbital Angular Momentum from HR 1895, Denis W. Oesch[1], Darryl J. Sanchez[2], Patrick R. Kelly[2]; [1]*Science Applications International Corp, USA;* [2]*AFRL, USA.* Observations of HR 1895 for photonic orbital angular momentum captured two significantly different signals in three separate measurements. Here we show the outlying point is a strong photonic orbital angular momentum signal.

PTu3F.5 • 16:10
Propagation of the Optical Rotational Correlation Field and Orbital Angular Momentum through Turbulence, Mazen Nairat[1], David Voelz[1]; [1]*New Mexico State University, USA.* We consider a general formulation that describes the propagation of the rotational correlation field through atmospheric turbulence. The associated influence on a spatial distribution of the orbital angular momentum of a single photon is analytically determined.

QTu3G • Diagnostic Optical Technologies—Continued

QTu3G.2 • 15:10
Numerical simulation of the influence of optical absorption of tumor on Laser induced ultrasonic in soft tissue, rongrong an[1], Xiaosen Luo[1], Zhonghua Shen[1]; [1]*School of Science, Nanjing Univ. of Science and Technology, China.* The use of a pulsed laser for the generation of the elastic waves in soft tissues containing tumors with different optical absorption in the thermoelastic regime is investigated through the finite element method and experiments.

QTu3G.3 • 15:30
High-Throughput Quantitative Fluorescence Lifetime Imaging based on Active Wide-Field Illumination, Lingling Zhao[1], Ken Abe[2], Margarida Barroso[2], Xavier Intes[1]; [1]*Rensselaer Polytechnic Inst., USA;* [2]*Albany Medical College, USA.* We developed an active illumination strategy to acquire fluorescence signals over large fluorophore concentration distributions. It can improve the SNR and weak-signal sensitivity for enhanced accuracy of lifetime estimation at high acquisition speed.

QTu3G.4 • 15:50
Determination of detection limitation of NIRF device using QDots 800 based fluorescent solid phantom, Banghe Zhu[1], John C. Rasmussen[1], Eva M. Sevick-Muraca[1]; [1]*UT Health Science Center, USA.* Solid fluorescent phantoms were constructed to assess detection limitations of investigational NIRF imaging devices. The phantoms enabled the quantitative assessment of the fluorescent status of lymph nodes following resection from breast cancer patients.

QTu3G.5 • 16:10
Quantitative Detection of Near Infrared-labeled Transferrin using FRET Fluorescence Lifetime Wide-Field Imaging in Breast Cancer Cells In Vitro and In Vivo, Ken Abe[1], Lingling Zhao[2], Xavier Intes[2], Margarida Barroso[1]; [1]*Cardiovascular Sciences, Albany Medical College, USA;* [2]*Biomedical Engineering, Rensselaer Polytechnic Inst., USA.* A novel near infrared FRET fluorescence lifetime imaging technique with wide-field illumination strategies was developed to validate and characterize cellular uptake of transferrin in both cancer cells and normal cells in vitro and in vivo. Joint Sessions

16:30–18:00
JTu4A • Joint Poster Session

JTu4A.1
Determination of the beam profile for the Herschel-SPIRE Imaging Fourier Transform Spectrometer, Gibion Makiwa[1], David A. Naylor[1], Marc Ferlet[2], Carl Salji[3], Bruce Swinyard[2,3], Edward Polehampton[1,2], Matthijs H. D. van der Wiel[1]; *[1]Department of Physics and Astronomy, Univ. of Lethbridge, Canada; [2]RAL Space, Rutherford Appleton Laboratory, UK; [3]Department of Physics and Astronomy, Univ. College London, UK.* The Herschel-SPIRE imaging Fourier Transform Spectrometer employs feed-horn coupled bolometers to provide imaging spectroscopy. We discuss the wavelength dependent beam of the individual SPIRE FTS detectors.

JTu4A.2
Comprehensive Analyses of the Spectra of Iron-group Elements, Gillian Nave[1], Craig J. Sansonetti[1]; *[1]National Inst of Standards & Technology, USA.* We summarize work at the National Inst. of Standards and Technology (NIST) to measure and analyse the spectra of iron-group elements using Fourier transform and grating spectroscopy.

JTu4A.3
Imaging Spectroscopy with the Herschel-SPIRE Imaging Fourier Transform Spectrometer, Gibion Makiwa[1], Matthijs H. D. van der Wiel[1], David A. Naylor[1], Brad Gom[1]; *[1]Univ. of Lethbridge, Canada.* The spectral imaging capabilities of the Herschel-SPIRE imaging Fourier Transform Spectrometer are discussed. The process of data reduction and results from sample observations are presented.

JTu4A.4
Commissioning of FTS-2, the SCUBA-2 Imaging Fourier Transform Spectrometer, Brad Gom[1], David A. Naylor[1], Per Friberg[2], Graham Bell[2]; *[1]Univ. of Lethbridge, Canada; [2]Joint Astronomy Centre, USA.* We present early results from the commissioning of FTS-2, the imaging Fourier transform spectrometer for use with SCUBA-2 at the James Clerk Maxwell Telescope.

JTu4A.5
Studies of the far IR water vapour continuum from CAVIAR and RHUBC campaigns using TAFTS, Cathryn Fox[1], Juliet C. Pickering[1], Paul D. Green[2], Ralph Beeby[1], Jonathan E. Murray[1], Alan Last[1]; *[1]Imperial College London, UK; [2]National Physical Laboratory, UK.* We report results from the participation of the Imperial College TAFTS instrument in the CAVIAR and RHUBC field campaigns, validating a derived water vapor continuum parameterization in the far-IR spectral region.

JTu4A.6
Application of solar SCIDAR technique to measuring wind velocity, Noriaki Miura[1], Ayumu Oh-ishi[1], Susumu Kuwamura[1], Naoshi Baba[2], Satoru Ueno[3], Kiyoshi Ichimoto[3]; *[1]Computer Sciences, Kitami Inst. of Technology, Japan; [2]Applied Physics, Hokkaido Univ., Japan; [3]Hida Observatory, Kyoto Univ., Japan.* We extend our solar SCIDAR technique to measuring wind velocities on turbulent layers. We apply our technique to observed data and confirm that peaks corresponding to wind flows appear on a temporal-correlation plane.

JTu4A.7
Single Wave-Front Sensor Control Many Deformable Mirrors: Theory and Experiment, Hongwei Ye[1], Feng Shen[1], Rui Zhou[1], DaoAi Dong[1], Yongdong Gan[1]; *[1]Inst. of Optics and Electronics, Chinese Academy of Sciences, China.* New kinds of real-time wavefront compensation algorithms were tested. The experiment data proved that the single wave-front sensor control double mirrors adaptive optical system could improve system performance in the same work condition.

JTu4A.8
Phase Contrast Method for Wave Front Sensing in Adaptive Optics; An Approach from Curvature Sensing, Masayuki Hattori[1]; *[1]Subaru Telescope, National Astronomical Observatory Japan, USA.* Phase contrast method sensible to the tip-tilt is configured by modification of the vibrating membrane in the curvature adaptive optics, with inheriting robustness by the differential measurement. The summary of the computer simulations are shown.

JTu4A.9
Comparison of Surface Shape Control Algorithms for Deformable Mirror, Tenghao Li[1], Lei Huang[1], Zexin Feng[1], Yuntao Qiu[1], Qiao Xue[1], Xingkun Ma[1], Gong Mali[1]; *[1]Department of Precision Instruments, Tsinghua Univ., China.* Two surface shape control algorithms for deformable mirror, direct slope control and reconstruction-based control, are analyzed and compared both theoretically and numerically. It is shown that the latter one generally performs better and more stable.

JTu4A.10
A Polarization Imagery Fusion Algorithm Based on NMF and PCNN, Siyuan Zhang[1], Yan Yuan[1], Lijuan Su[1], Liang Hu[1]; *[1]Key Laboratory of Precision Opto-mechatronics Technology, Ministry of Education, Beihang Univ., China.* Introduce a polarization imagery fusion algorithm based on non-negative matrix factorization and pulse coupled neural network. The presented algorithm yields image with much higher quality and preserves more detail information of the objects.

JTu4A.11
Two Dimensional Phase Unwrapping for Coherent Imaging, Neal Bambha[1], Justin Bickford[1], Karl Klett[1]; *[1]US Army Research Laboratory, USA.* We describe a phase unwrapping algorithm for digital holographic images. The algorithm uses preprocess smoothing, phase gradient calculations, and amplitude measures to determine the reliability of a given data point, and follows a non-continuous path.

JTu4A.12
Deconvolution of Multiple Spectral Lines Shapes by Means of Tikhonov's Regularization Method, Gita Revalde[1,2], Natalja Zorina[2], Atis Skudra[2]; *[1]Inst. of Technical Physics, Riga Technical Univ., Latvia; [2]Insitute of Atomic Physics and Spectroscopy, Univ. of Latvia, Latvia.* We present deconvolution of multiple narrow Zeeman split Hg lines, emitted from Hg/Xe micro-size capillary and measured by the Fourier Transform spectrometer. The ill-posed inverse problem was solved using the Tikhonov's regularization method.

JTu4A.13
Modeling the Effect of Wave-front Aberrations in Fiber-based Scanning Optical Microscopy, Hans Verstraete[1], Michel Verhaegen[1], Jeroen Kalkman[1]; *[1]Delft Center for Systems and Control, Delft Univ. of Technology, Netherlands.* In scanning microscopy and optical coherence tomography, aberrations of the wave-front cause a loss in intensity and resolution. Intensity and resolution are quantified using Fresnel propagation, Fraunhofer diffraction, and the calculation of overlap integrals.

JTu4A.14
Phase imaging via compressive sensing, Pere Clemente[1,2], Vicente Durán[1,3], Pedro Andrés[4], Mercedes Fernández-Alonso[1,3], Enrique Tajahuerce[1,3], Jesús Lancis[1,3]; *[1]Departament de Física, Universsitat Jaume I, Spain; [2]Servei Central d'Instrumentació Científica, Universsitat Jaume I, Spain; [3]Institut de Noves Tecnologies de la Imatge, Universsitat Jaume I, Spain; [4]Departament d'Òptica, Universitat de València, Spain.* This communication develops a novel framework for phase imaging at optical wavelength by merging digital lenless phase-shifting holography with single-pixel optical imaging based on compressive sensing.

JTu4A.15
Single-pixel spectropolarimetric imaging by compressive sensing, Fernando Soldevila[1], Esther Irles[1], Vicente Durán[1,2], Pere Clemente[1,3], Mercedes Fernández-Alonso[1,2], Enrique Tajahuerce[1,2], Jesús Lancis[1,2]; *[1]Departament de Física, Universitat Jaume I, Spain; [2]Institut de Noves Tecnologies de la Imatge (INIT), Universitat Jaume I, Spain; [3]Servei Central d'Instrumentació Científica, Universitat Jaume I, Spain.* We present a single-pixel camera that performs polarimetric multispectral imaging by applying the theory of compressive sensing. For different spectral channels, we obtain polarimetric images that provide information about the spatial distribution of light polarization.

JTu4A.16
Inverse Electromagnetic Design for Imaging, Vidya Ganapati[1], Samarth Bhargava[1], Eli Yablonovitch[1]; *[1]Univ. of California, Berkeley, USA.* We describe an inverse electromagnetic design algorithm to design computer generated holograms in the full-wave domain, with a finite-difference time-domain solver. The algorithm searches for an optimal binary hologram design with the adjoint gradient method.

JTu4A.17
Phase Diversity Implementation in Fresnel Incoherent Holography, Iftach Klapp[1], Joseph Rosen[1]; *[1]Electrical and Computer Engineering, Ben Gurion Univ. of the Negev, Israel.* A new adaptive implementation of the Fresnel incoherent correlation holography (FINCH) is presented. By implementing phase diversity mechanism, we allow wavefront error compensation without the need of a guide star. Simulation results present significant resolution improvement.

JTu4A.18
Condition number in recovery of signals from partial fractional Fourier domain information, Figen S. Oktem[1], Haldun M. Ozaktas[2]; *[1]Univ of Illinois at Urbana-Champaign, USA; [2]Bilkent Univ., Turkey.* The problem of estimating unknown signal samples from partial measurements in fractional Fourier domains arises in wave propagation. Using the condition number of the inverse problem as a measure of redundant information, we analyze the effect of the number of known samples and their distributions.

JTu4A.19
Modeling light propagation in transmission and backscattering optical coherence tomography, V. Duc Nguyen[1], Dirk J. Faber[1], Edwin van der Pol[1], Ton G. van Leeuwen[1], Jeroen Kalkman[2,1]; *[1]Biomedical Engineering & Physics, Academic Medical Center, Netherlands; [2]Delft Center for Systems and Control, TU Delft, Netherlands.* Concentration dependent scattering coefficients are measured using transmission optical coherence tomography (OCT) and compared to a dependent scattering model. The backscattering OCT signal is fitted with the extended Huygens-Fresnel model. Both models give good results.

JTu4A.20
Fluorescence holography with enhanced interference extent and improved signal-to-noise, Xiaomin Lai[1,2], Yiming Guo[1,2], Shaoqun Zeng[1,2]; *[1]Wuhan National Lab for Optoelectronics, China; [2]Department of Biomedical Engineering, China.* We present a system that can realize near focal plane detection with high extent of interference. The SNR is improved by about three times and a signal 4.6 times weaker can be detected.

JTu4A.21
Liquid Drop Lenses for Miniature Sensors, Brian McCall[1], Sri Rama Prasanna Pavani[1]; *[1]Ricoh Innovations, Inc., USA.* We introduce a lens fabrication method for computational imagers with on-contact dispensing of high-viscous UV curable epoxies on planar substrates. We further model and calibrate these lenses, and demonstrate applications in stereo and multi-aperture imaging.

JTu4A.22
Information Optimal Adaptive Measurement Design For Compressive Imaging, James Huang[1], Amit Ashok[2,1], Mark Neifeld[1,2]; *[1]Electrical and Computer Engineering, Univ. of Arizona, USA; [2]College of Optical Sciences, Univ. of Arizona, USA.* We design an adaptive compressive imager by maximizing mutual information between measurements and the object. Simulation result shows that the proposed design requires 1.5 times fewer measurements relative to a static information-optimal design.

JTu4A • Joint Poster Session—Continued

JTu4A.23
Restoration Method for Fiber Bundle Microscopy Using Interpolation Based on Overlapping Self-Shifted Images, Cheon-Yang Lee[1], Yeong-Mun Cha[1], Jae-Ho Han[1]; [1]*Korea Univ., Republic of Korea.* A method for restoring fiber bundle microscopy incorporating honeycomb artifact is demonstrated based on interpolating pixels using overlapped images. The imaging result with biological specimen shows improved image quality with minimally degraded sharpness as well.

JTu4A.24
Fiber Scanning Array for 3 Dimensional Topographic Imaging, Barry Coyle[1], David Rabine[1], Demetrios Poulios[2], Bryan Blair[1], Paul R. Stysley[1], Richard Kay[2], Greg Clarke[2], Jack Bufton[3]; [1]*NASA Goddard Space Flight Center, USA;* [2]*Physics, American Univ., USA;* [3]*Global Science Tech, USA.* This design presented is a 35 beam switched fiber optic array 3-D LIDAR . The instrument distributes ns pulses over a target and assembles the returns into 3-D images for Earth and planetary altimetry.

JTu4A.25
The optimization of PPIX formation at different skin layers using ALA evaluated by widefield fluorescence imaging and fluorescence spectroscopy, Priscila Menezes[1]; [1]*Optics, IFSC- USP, Brazil.* The PDT using 5-ALA as precursor of PPIX, have been used in the skin cancer treatment. This work aim evaluates the influence of negative pressure induction in the PPIX formation using imaging and spectroscopy fluorescence analyses.

JTu4A.26
Single Sensor Stereoscopic Camera for Robot Navigation, Chang-Woo Park[1], Sewoong Jun[1]; [1]*Korea Electronics Technology Inst., Republic of Korea.* This paper presents a new stereoscopic camera system to acquire depth information from robot operating environments with obstacles, human bodies, and home facilities.

JTu4A.27
Improving retinal images by model based ocular point spread function estimation, Nizan Meitav[1], Erez N. Rbiak[1]; [1]*Physics, Technion - Israel Inst. of Technology, Israel.* In vivo retinal imaging often suffers from blurring aberrations. We demonstrate a method to enhance the contrast of retinal cells by estimating the ocular PSF. This is done by retinal cells' modeling.

JTu4A.28
Aperture design in wedge projection display for on-axis imaging system, Chang-Kun Lee[1], Youngmo Jeong[1], Sung-Wook Min[2], Byoungho Lee[1]; [1]*School of Electrical Engineering, Seoul National Univ., Republic of Korea;* [2]*Department of Information Display, Kyung Hee Univ., Republic of Korea.* We analyze the relation between the aperture and waveguide parameters. We derive the numerical equation for on-axis imaging with prism structure. Experimental results show that proposed structure enhances image quality and expands expressible area.

JTu4A.29
Multi-parameter Sensing Based on Graded-index multimode fiber, Jianzhong Zhang[1]; [1]*Harbin Engineering Univ., China.* We demonstrate a smart optical fiber sensor unit, based on combing a Bragg grating in graded-index multimode fiber and a Fizeau cavity, to realize a multi-parameter sensing of temperature, curvature and strain or displacement.

JTu4A.30
Development of a Fast Measurement System for Microstructured Surfaces, Renke Scheuer[1], Thomas Mueller[1], Eduard Reithmeier[1]; [1]*Inst. of Measurement and Automatic Control, Leibniz Univ. Hannover, Germany.* This paper describes the development of a measurement system for fast analysis of microstructured surfaces. The main component is a high-speed video camera with a telecentric lens. Measurement speed of 1000 mm²/min can be achieved.

JTu4A.31
Dynamic phase profile of a thin flame using a single-shot polarizing phase shifting interferometry, Noel-Ivan Toto-Arellano[1], David Serrano-García[2], Luis García-Lechuga[1], Juan Marcelo Miranda Gómez[1], German Resendiz López[1], Angelina González Rosas[1]; [1]*Óptica y Fotónica, Universidad Tecnológica de Tulancingo, Mexico;* [2]*Laboratorio de Metrología III, Centro de Investigaciones en Óptica, A.C, Mexico.* In this paper, we propose a Quasi Common-Path Interferometer based on a two beams configuration using simultaneous phase shifting interferometry modulated by polarization that shows insensitivity against external vibration. Experimental results are also given.

JTu4A.32
3-D Optical Metrology of Finite sub-20 nm Dense Arrays with sub-nanometer Parametric Uncertainties, Jing Qin[1], Hui Zhou[1], Bryan Barnes[1], Ronald Dixson[1], Richard M. Silver[1]; [1]*Semiconductor and Dimensional Metrology Division, NIST, USA.* A new approach that involves parametric fitting of 3-D scattered field with electromagnetic simulation, Fourier domain normalization, and uncertainties analysis is presented to rigorously analyze 3-D through-focus optical images of targets that scatter a continuum of frequency components

JTu4A.33
Random optical scatter filters for spectrometers: Implementation and Estimation, Woong-Bi Lee[1], Oliver James[1], Seung-Chul Kim[2], Heung-No Lee[1]; [1]*Department of Information and Communications, Gwangju Inst. of Science and Technol, Republic of Korea;* [2]*Gmeric, Republic of Korea.* In this paper, we introduce an implementation of filters with random transmittance for miniature spectrometers with limited number of CCD elements. We also present a method for estimating the random transmittances, which are needed for recovering the signal spectrum.

NOTES

Random optical scatter filters for spectrometers: Implementation and Estimation

Woong-Bi Lee, J. Oliver, Seung-Chul Kim, and Heung-No Lee*
School of Information and Communications, Gwangju Institute of Science and Technology, South Korea.
*wblee@gist.ac.kr, oliver@gist.ac.kr, kscmail@hanmail.net, heungno@gist.ac.kr**

Abstract: In this paper, we introduce an implementation of filters with random transmittance for miniature spectrometers with limited number of CCD elements. We also present a method for estimating the random transmittances, which are needed for recovering the signal spectrum.
OCIS codes: (300.6320) Spectroscopy, high-resolution; (120.2440) Instrumentation, measurement, and metrology, filters

1. Summary

Miniature spectrometers play a major role in various academic and industrial applications such as bio-medical, chemical, and environmental engineering [1]. A family of spectrometers that are built with an array of optical filters offers miniaturization, superior portability, and cost effectiveness [2]. The spectrometers measure properties of light source over various spectral components [3].

The state of the art filter-array based spectrometers are equipped with digital signal processing (DSP) algorithms to alleviate distortions and to reconstruct the original signal spectrum. The resolving ability of these spectrometers is determined by the number of filters in the filter array and the shapes of the transmittance functions (TF) of these filters [4]. In practice, due to low-cost integrated-array fabrication, the number of filters in miniature spectrometers is fixed (and hence the CCD elements) and the shape of the TF of each of the filters is non-ideal as in [5]. A signal spectrum passing through these non-ideal filters is severely distorted. Hence, digital signal processing of the spectrum measured by the spectrometer is necessary. In [5], the L_1 norm minimization-based DSP algorithm is used for processing the signal spectrum obtained from the spectrometer. In [6], filters with random TFs are proposed that was used along with the DSP algorithm in [5] for recovering the input signal spectrum. The random filters have two main properties. First, the transmittance of a filter at one wavelength is completely different and uncorrelated with that at the other wavelength. Second, the shape of each filter's transmittance is uncorrelated with other filters in the filter-array. With these random TFs, in [6], a mercury signal spectrum was shown to be successfully recovered better than using filters with non-ideal TFs in [5]. However, in [6], the TFs of random filters are generated by randomly varying the thickness of the layers in thin-film filters.

In this paper, we propose a new implementation of the random transmittance filter-array by attaching scatter filters with random TFs to the existing grating in a spectrometer. Our approach is different from [6] in that now the estimation of the random TFs is necessary to recover the original signal spectrum using the DSP. We estimate the random TFs by modeling the raw spectrum from the spectrometer and show through real world experiments that random filters can be implemented and aid in the recovery of an input signal spectrum.

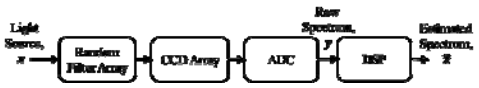

Fig. 1. Schematic of the proposed filter-array based spectrometer

We consider a spectrometer that consists of a planar filter array (filter elements attached to a grating) with M filters and its corresponding CCD array as shown in Fig. 1. Each filter randomly selects (transmits) the input wavelength components which are recorded by the CCD. The output of the CCD is sampled in analog-to-digital converter (ADC) and fed into a DSP unit to estimate the spectrum. The data model for the raw spectrum, $\boldsymbol{y} \in \mathbb{R}^{M\times 1}$, which is an input to the DSP algorithm can be represented as a system of linear equations:

$$\boldsymbol{y} = \boldsymbol{D}\boldsymbol{x} + \boldsymbol{w}, \qquad \boldsymbol{x} \geq 0 \qquad (1)$$

where the $N \times 1$ vector $\boldsymbol{x}$ contains the samples of the original signal spectrum, the matrix $\boldsymbol{D}$ is an $M \times N$ TF matrix, and $\boldsymbol{w}$ is $M \times 1$ noise vector. Each row of D is a TF of a filter. Since the number of spectral components of $\boldsymbol{x}$ is greater than the number of filters, the value of N is greater than M, i.e., $N > M$.

In order to estimate TFs, we observe L number of raw spectrum by applying monochromatic light sources with various wavelengths. The observed L raw spectrums can be put together as a single matrix equation as

$$\boldsymbol{Y} = \boldsymbol{DX} + \boldsymbol{W} \quad \text{where} \quad \boldsymbol{X} \geq 0 . \tag{2}$$

where the matrix $\boldsymbol{X}$ is $N \times L$ input signal spectrum whose columns are signal spectrum of various light sources , the matrix $\boldsymbol{Y}$ is $M \times L$ raw spectrum, and $\boldsymbol{W}$ is $M \times L$ noise matrix. The goal of the TF estimator is to obtain an estimate $\widehat{D} \in \mathbb{R}^{M \times N}$ of D from the raw spectrum $\boldsymbol{Y}$, given the matrix $\boldsymbol{X}$. We obtain the estimate $\widehat{D}$ as

$$\widehat{\boldsymbol{D}} = \boldsymbol{Y} \cdot \mathrm{pinv}\left(\boldsymbol{X}\right) \tag{3}$$

where $\mathrm{pinv}(\cdot)$ represents the pseudo-inverse .

Once we obtain the TFs of the random filters, we rewrite Eq. (1) using sparse representation. Any natural signal or a vector $\boldsymbol{x}$ in Eq. (1) can be represented as sparse in a certain basis, i.e., $\boldsymbol{x} = \boldsymbol{Gs}$. The basis $\boldsymbol{G} \in \mathbb{R}^{N \times N}$ is called kernel matrix and the signal $\boldsymbol{s} \in \mathbb{R}^{N \times 1}$ is K-sparse vector, i.e., only K components of $\boldsymbol{s}$ are non-zero values and $N - K$ components are zero, where $K << N$. Each column of the matrix $\boldsymbol{G}$ contains spectrum of a monochromatic light sources. That is, any signal spectrum can be represented by linear combinations of monochromatic light sources. With the sparse representation of the input signal spectrum, Eq. (1) can be rewritten as

$$\boldsymbol{y} = \underbrace{\boldsymbol{DG}}_{\boldsymbol{A}} \boldsymbol{s} + \boldsymbol{w} = \boldsymbol{A}\boldsymbol{s} + \boldsymbol{w} \quad \text{where} \quad \boldsymbol{s} \geq 0 . \tag{4}$$

The DSP algorithm aims to obtain an estimate $\hat{\boldsymbol{s}}$ of $\boldsymbol{s}$ from the raw spectrum $\boldsymbol{y}$, given the estimated TF matrix and $\boldsymbol{G}$.

A recovery algorithm in [6] is based on a DSP optimization tool called L_1 norm minimization. The L_1 norm minimization for the recovery of the sparse signal $\boldsymbol{s}$ in Eq. (4) can be expressed as

$$\hat{\boldsymbol{s}} = \min_{s} \left\| \boldsymbol{s} \right\|_1 \quad \text{subject to} \quad \left\| DG\boldsymbol{s} - \boldsymbol{y} \right\|_2 \leq \varepsilon, \ \ \boldsymbol{s} \geq 0 \tag{5}$$

where ε is a small positive constant.

In the experiment, we have solved the problem in Eq. (5) for sparse signal recovery. We implement a filter-based spectrometer with following parameters: M = 40, N = 800, and L = 255.

As shown in Fig. 2, we generate 255 numbers of monochromatic light sources range from 428 nm to 682 nm. A monochromatic light source is divided into two sources. One is inserted into a spectrometer with random transmittance and the output $\boldsymbol{y}$ is obtained. The other is inserted into a high resolution spectrometer which measure the input signal spectrum $\boldsymbol{x}$. We repeat this experiment for L times with different monochromatic light sources in order to model the raw spectrum as in Eq. (2) and estimate $\widehat{D}$ as per Eq. (3).

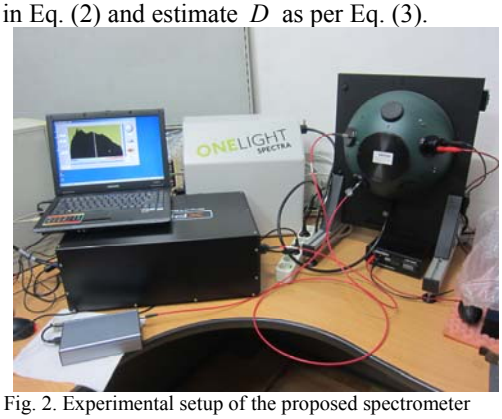

Fig. 2. Experimental setup of the proposed spectrometer

Three of the estimated TFs are shown in Fig. 3. Each random filter captures holistic and independent information about the signal spectrum.

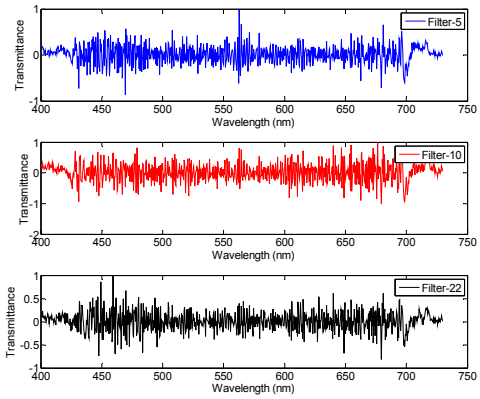

Fig. 3. Estimated random transmittances

With the estimated TFs, $\widehat{D}$, we verify the ability of the spectrometer with only 40 CCD elements in recovering the fluorescent light spectrum of 3 dominant wavelengths. As shown in Fig. 4, the spectrometers with random filter array can detect three distinct peaks of the source. We did not do much to the effect of noise in Eq. (2) and (4). In our future work, we aim to measure the statistical properties of the noise and use them to improve the results.

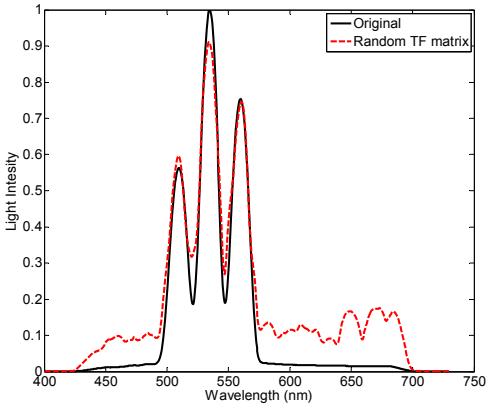

Fig. 4. Reconstruction of fluorescent light of 3 wavelengths

In conclusion, we have shown that the optical filters with random TFs in [6] can be implemented in the real world by placing randomly scattering filters between gratings and CCD array. The role of random filters is to acquire global information about the signal spectrum, rather than localized information which was the target of traditional designs. The set of global information captured by each filter helps the DSP algorithm to recover the input signal spectrum in detail. We demonstrated through experiments the signal spectrum recovering ability of the proposed random filters after estimating their transmittances.

Acknowledgement

This work was supported by the National Research Foundation of Korea (NRF) grant funded by the Korean government (MEST) (Do-Yak Research Program, No. 2012-0005656)

4. References

[1] D. J. Brady, *Optical Imaging and Spectroscopy* (John and Wiley Sons, 2009)
[2] S. W. Wang, C. Xiz, X. Chen, and W. Lu. "Concept of a high-resolution miniature spectrometer using an integrated filter array," Opt. Lett. 32, 632-634 (2007).
[3] W. L. Wolfe, *Introduction to Imaging Spectrometers* (SPIE, 1997).
[4] H. N. Lee, Introduction to Compressed Sensing (Lecture notes; Spring Semester, GIST, Korea, 2011). http://infonet.gist.ac.kr/wp-content/uploads/2012/11/Book_CS.pdf
[5] J. Oliver, W. B. Lee, S. J. Park, and H. N. Lee, "Improving resolution of miniature spectrometers by exploiting sparse nature of signals," Opt. Exp. 20, 2613-2625 (2012).
[6] J. Oliver, W. B. Lee, and H. N. Lee, "Filters with random transmittance for improving resolution in filter-array-based spectrometers," Opt. Exp. 21, 3969-3989 (2013).